Eur. Phys. J. B **49**, 283–287 (2006)
DOI: 10.1140/epjb/e2006-00077-1

THE EUROPEAN PHYSICAL JOURNAL B

Jordan-Wigner approach to the frustrated spin one-half XXZ chain

T. Verkholyak[1,a], A. Honecker[2], and W. Brenig[2]

[1] Institute for Condensed Matter Physics, 1 Svientsitskii Str., L'viv-11, 79011, Ukraine
[2] Technische Universität Braunschweig, Institut für Theoretische Physik, Mendelssohnstrasse 3, 38106 Braunschweig, Germany

Received 16 November 2005 / Received in final form 6 January 2006
Published online 10 March 2006 –

Abstract. The Jordan-Wigner transformation is applied to study the ground state properties and dimerization transition in the $J_1 - J_2$ XXZ chain. We consider different solutions of the mean-field approximation for the transformed Hamiltonian. Ground state energy and the static structure factor are compared with complementary exact diagonalization and good agreement is found near the limit of the Majumdar-Ghosh model. Furthermore, the ground state phase diagram is discussed within the mean-field theory. In particular, we show that an incommensurate ground state is absent for large J_2 in a fully self-consistent mean-field analysis.

PACS. 75.10.Jm Quantized spin models – 75.30.Kz Magnetic phase boundaries (including magnetic transitions, metamagnetism, etc.) – 75.40.Mg Numerical simulation studies

1 Introduction

Low-dimensional quantum spin systems with competing interaction are a field of diverse theoretical studies [1]. Recent progress in material synthesis has brought up several transition metal oxides realizing such spin systems. In particular, the $s = 1/2$ spin chain with frustrated next-nearest neighbor interaction has been found to model the quasi one-dimensional copper oxide material $CuGeO_3$ [2,3]. The $J_1 - J_2$ Heisenberg chain is well known to display a quantum phase transition from a gapless, translationally invariant ground state with algebraic spin-correlations to a dimer state [4] at $J_2 \approx 0.24 J_1$ [5,6]. At the Majumdar-Ghosh point [7], i.e. at $J_2 = J_1/2$, the ground state is a doubly degenerate dimer product of singlet pairs on neighboring sites. In the vicinity of the Majumdar-Ghosh point there is a transition [8] to an incommensurate phase for larger J_2 [5,9]. Low-energy field theories [5,10] are not suitable for describing this transition since it occurs at a very short correlation length of about one lattice spacing. Also semiclassical approaches [11,12] are not applicable to this commensurate-incommensurate transition in the $J_1 - J_2$ chain with $s = 1/2$, since they fail to reproduce e.g. the solitonic nature of the fundamental excitations [13].

The Jordan-Wigner transformation is another technique which allows for an approximate analytic analysis of low-dimensional quantum spin systems (see e.g. Ref. [14] for a recent review). It has also been applied to the $J_1 - J_2$ chain [15,16], however only for a restricted set of mean-field configurations. While reference [16] reported incommensurability for larger J_2, this work did not consider dimerized states and thus fails to reproduce the gap which is known to be relevant in this region (see e.g. [5]). This motivates us to perform a systematic study of the spin-1/2 $J_1 - J_2$ chain using the Jordan-Wigner transformation and considering all possible mean-field configurations. Since the Jordan-Wigner transformation is known to be exact for the nearest-neighbor XY chain [17], we will further consider the case of a general XXZ anisotropy. Note that the effects of the anisotropy in the spin-1/2 $J_1 - J_2$ chain have been studied systematically either numerically [18,19] or using field theoretical approaches [4,20,21], but not in previous Jordan-Wigner treatments [15,16].

This paper is organized as follows: in Section 2 we perform a mean-field analysis of the Jordan-Wigner transformed [22,23] Hamiltonian. Remarkably, the Majumdar-Ghosh state [7,24] is recovered exactly by our approach. Section 3 presents results obtained from a numerical solution of the mean-field equations and a comparison with complementary exact diagonalization data. Finally, Section 4 summarizes our results concerning in particular the applicability of the Jordan-Wigner approach to the different parameter regimes.

[a] e-mail: werch@icmp.lviv.ua

2 Mean-field analysis

In the following we consider the frustrated spin-1/2 XXZ chain of L spins ($L \to \infty$):

$$H = \sum_{l=1}^{L} J_1(s_l^x s_{l+1}^x + s_l^y s_{l+1}^y + \Delta s_l^z s_{l+1}^z) + J_2(s_l^x s_{l+2}^x + s_l^y s_{l+2}^y + \Delta s_l^z s_{l+2}^z). \quad (1)$$

Here J_1 (J_2) > 0 is the nearest (next-nearest) neighbor coupling, Δ is the exchange anisotropy and s_l^α are spin-1/2 operators. By the Jordan-Wigner transformation [22,23] the spin Hamiltonian (1) is mapped onto a model of interacting spinless fermions $c_l^{(+)}$:

$$H = \sum_{l=1}^{L} \left(\frac{J_1}{2} c_l^+ c_{l+1} + \frac{J_2}{2} c_l^+ c_{l+2} - J_2 c_l^+ c_{l+1}^+ c_{l+1} c_{l+2} + \text{h.c.} \right) + \Delta J_1 \left(c_l^+ c_l - \frac{1}{2} \right) \left(c_{l+1}^+ c_{l+1} - \frac{1}{2} \right) + \Delta J_2 \left(c_l^+ c_l - \frac{1}{2} \right) \left(c_{l+2}^+ c_{l+2} - \frac{1}{2} \right). \quad (2)$$

The first term corresponds to the XY nearest-neighbor interaction and can be treated rigorously [25]. The remaining terms are the z component of the nearest neighbor and the complete next-nearest neighbor exchange. They represent four-fermion interactions which render the model non-integrable. We will therefore resort to a mean-field approximation preserving all pair correlations of type $\langle c_n^+ c_m \rangle$ in the factorization of the interaction terms:

$$\begin{aligned} g_l &= \langle s_l^z \rangle = \langle c_l^+ c_l \rangle - \frac{1}{2}, \\ A_l &= \langle c_l^+ c_{l+1} \rangle = \langle c_{l+1}^+ c_l \rangle, \\ D_l &= \langle c_l^+ c_{l+2} \rangle = \langle c_{l+2}^+ c_l \rangle. \end{aligned} \quad (3)$$

These contractions are related to single-site, nearest neighbor, and next-nearest neighbor spin-spin correlation functions. The self-consistent determination of these contractions follows reference [15], where however only the case of $g_l = D_l = 0$ had been considered. We find the following phases:

i) paramagnetic (*homogeneous*) [26]: $A_l = A = -\frac{1}{\pi}$, $g_l = D_l = 0$;
ii) uniform antiferromagnetic (*AFM+uni.*): $g_l = (-1)^l g$, $A_l = A$, and $D_l = D$;
iii) staggered antiferromagnetic (*AFM+stag.*): in contrast to ii) D_l is staggered, i.e. $D_l = (-1)^l D$;
iv) alternating nearest neighbor hopping (*dimer*): $A_l = A + (-1)^l \delta$.

The self-consistency equations for phase iv) are discussed below. Here, we should only note that in all cases we find no uniform contribution to the next-nearest neighbor correlation D_l. A staggered next-nearest neighbor contraction is induced by the antiferromagnetic order and tends to zero when $g = 0$. Therefore, the current mean-field approach is not suited to treat the limit of two weakly coupled chains ($J_1 \to 0$) where the correlation between the next-nearest neighbor spins becomes strongest.

For case iv), and after Fourier transformation the mean-field Hamiltonian reads

$$H = \sum_{-\pi < k \le \pi} e_k \, c_k^+ c_k + \frac{i f_k}{2} (c_{k\pm\pi}^+ c_k - c_k^+ c_{k\pm\pi}), \quad (4)$$

where $e_k = (J_1 - 2A(\Delta J_1 - 2J_2))\cos(k)$, $f_k = 2\delta(\Delta J_1 + 2J_2)\sin(k)$. The Hamiltonian can be diagonalized by the unitary transformation

$$\begin{aligned} c_k &= \frac{1+i}{\sqrt{2}} (\cos(\alpha_k/2)\, \eta_k - \sin(\alpha_k/2)\, \eta_{k\pm\pi}), \\ c_{k\pm\pi} &= \frac{1-i}{\sqrt{2}} (\sin(\alpha_k/2)\, \eta_k + \cos(\alpha_k/2)\, \eta_{k\pm\pi}), \end{aligned}$$

where $\cos\alpha_k = e_k/\sqrt{e_k^2+f_k^2}$. This leads to the free fermion model

$$H = \sum_{-\frac{\pi}{2} < k \le \frac{\pi}{2}} \lambda_k \left(\eta_k^+ \eta_k - \eta_{k\pm\pi}^+ \eta_{k\pm\pi} \right), \quad (5)$$

with the spectrum: $\lambda_k = \sqrt{e_k^2 + f_k^2}$. For the selfconsistent equations for A, δ we find:

$$\begin{aligned} A &= -\frac{1}{2\pi} \int_{-\frac{\pi}{2}}^{\frac{\pi}{2}} dk \, \cos(k) \frac{e_k}{\sqrt{e_k^2 + f_k^2}}, \\ \delta &= \frac{1}{2\pi} \int_{-\frac{\pi}{2}}^{\frac{\pi}{2}} dk \, \sin(k) \frac{f_k}{\sqrt{e_k^2 + f_k^2}}. \end{aligned} \quad (6)$$

The mean-field approximation to the ground-state energy is obtained from the ground state expectation value of the fermion Hamiltonian (2), including contractions only up to quadratic order. For the dimer phase iv) the ground state energy per site is

$$e = J_1 A - (\Delta J_1 - 2J_2) A^2 - (\Delta J_1 + 2J_2)\delta^2. \quad (7)$$

We note that the dimer order parameter [5] $d = \langle \boldsymbol{S}_{2i-1} \boldsymbol{S}_{2i} \rangle - \langle \boldsymbol{S}_{2i} \boldsymbol{S}_{2i+1} \rangle$ corresponds to $4(A-1)\delta$ within our treatment.

So far, we have assumed that the mean fields are real. However, it is known that an easy-plane anisotropy $\Delta < 1$ induces a chiral phase for large J_2 [10,27] (note that the existence of such a chiral phase had been verified numerically in a different ladder model [28] prior to [27]). The chiral order parameter $\kappa_l = s_l^x s_{l+1}^y - s_l^y s_{l+1}^x$ corresponds to the imaginary part of the fermion nearest-neighbor contraction $\Im\mathrm{m} A_l$. Therefore, the elementary contraction should be allowed to be complex. In this case the ground state energy reads:

$$\begin{aligned} e = {} & J_1 A_R - (\Delta J_1 - 2J_2) A_R^2 - (\Delta J_1 + 2J_2)\delta_R^2 \\ & - (\Delta J_1 + 2J_2) A_I^2 - (\Delta J_1 - 2J_2)\delta_I^2. \end{aligned} \quad (8)$$

Here $A_{R(I)}$ is the real (imaginary) part of A, and $\delta_{R(I)}$ is the real (imaginary) part of δ. It is evident that for

large J_2/J_1 a non-zero A_I lowers the ground state energy in contrast to δ_I. Hence, we have considered mean-field solutions with non-zero A_R, A_I, and δ_R. However, numerical solution of the mean-field equations did not yield any complex solution.

The Majumdar-Ghosh point [7,24] $J_2 = J_1/2$ permits to check the consistency of the mean-field approximation. At this point the ground state is doubly degenerate and consists of singlet pairs on neighboring sites $\prod_{l=1}^{N/2}[2l \mp 1, 2l]$, where $[2l \mp 1, 2l]$ denotes one singlet. This can be related to the fermion language by recalling that $S^z = +(-)1/2$ on site l corresponds to a filled (empty) site l. Therefore $(c^+_{2l\mp1} - c^+_{2l})|0\rangle$ creates a singlet bond on neighboring sites $2l \mp 1$, $2l$, and the Majumdar-Ghosh states can be represented [29] as $\prod_{l=1}^{N/2}(c^+_{2l\mp1} - c^+_{2l})|0\rangle$. We will now argue that this exact state is also obtained from the mean-field solution. For $J_2 = J_1/2$ configuration iv) and equation (6) yield $A = -1/4$, $\delta = \pm 1/4$. Inserting this solution into the mean-field Hamiltonian one gets

$$H = \sum_{l=1}^{N/2} \frac{J_1(1+\Delta)}{2}(\eta_l^{(t)+}\eta_l^{(t)} - \eta_l^{(s)+}\eta_l^{(s)}) + \frac{NJ_1\Delta}{8}, \quad (9)$$

where $\eta_l^{(t)} = \frac{1}{\sqrt{2}}(c_{2l\mp1} + c_{2l})$, $\eta_l^{(s)} = \frac{1}{\sqrt{2}}(c_{2l\mp1} - c_{2l})$ for $\delta = \pm\frac{1}{4}$. $\eta_l^{(s)+}$ and $\eta_l^{(s)}$ ($\eta_l^{(t)+}$ and $\eta_l^{(t)}$) create and annihilate a singlet (triplet) on nearest neighbors. This shows that the mean-field solution is the Majumdar-Ghosh state in fermionic representation $\prod_{l=1}^{N/2}\eta_l^{(s)+}|0\rangle$ with the ground state energy per spin $e = -J_1(2+\Delta)/8$.

3 Results

Figure 1 shows results of a numerical solution of the self-consistency equations for configurations i)–iv). It can be seen that all solutions exist for positive J_2. To check the accuracy of these results, we have performed exact diagonalization of the Hamiltonian (1) for $L \le 32$ sites (since this type of computations has a long tradition [30], similar results can also be found in the literature, in particular for $\Delta = 1$). We have performed a finite-size extrapolation using the Vanden-Broeck-Schwartz-algorithm [31] with $\alpha_{\rm VBS} = -1$ and, for most cases, $L = 12, 16, \ldots 32$. The extrapolated results for the ground-state energy per site e are shown by the circles in Figure 1. Errors are estimated to be smaller than the size of the symbols. For $J_2 = 0$, our extrapolated values agree to better than $10^{-6}J_1$ with the exact answer [17] $e/J_1 = -1/\pi \approx -0.318310$ and $1/4 - \ln(2) \approx -0.443147$ for $\Delta = 0$ and 1, respectively.

Apart from the exact ground state at the Majumdar-Ghosh point we may contrast the mean-field solutions against other known results. We start from the XY nearest-neighbor model ($\Delta = 0$, $J_2 = 0$) where the Jordan-Wigner transformation yields the exact answer [17]. For small J_2/J_1 the results of all approximations are very close (upper panel of Fig. 1) and all order parameters grow very slowly. In fact, a detailed analysis of equation (6) for A, δ shows that $J_2 > J_{2,\rm dim} = -\Delta J_1/2$

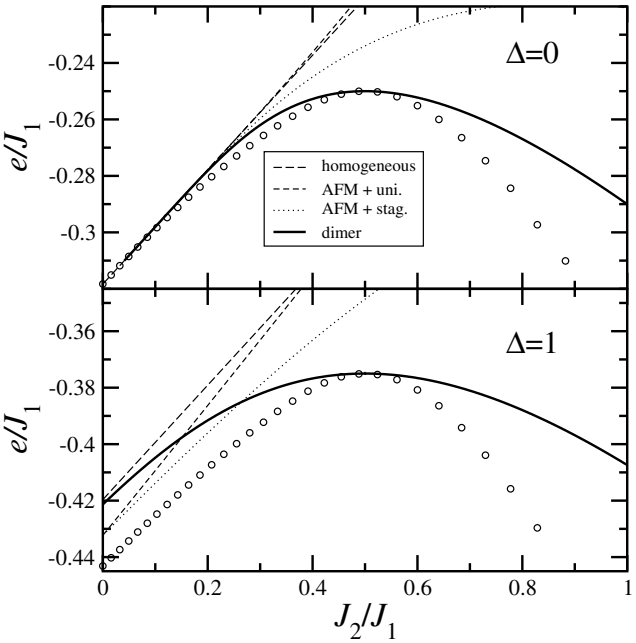

Fig. 1. Ground-state energy per site as a function of J_2/J_1 for the $J_1 - J_2$ XY chain (upper panel) and the Heisenberg chain (lower panel): the circles are exact diagonalization data extrapolated to the infinite system; lines correspond to the different mean-field solutions for the ground state.

is the condition of a non-zero solution for δ. The approximate solution for small $J_2 - J_{2,\rm dim}$ above this point gives

$$\delta \approx \frac{a}{e(J_2 - J_{2,\rm dim})} \exp\left(-\frac{\pi a}{4(J_2 - J_{2,\rm dim})}\right), \quad (10)$$

where $a = J_1 - \frac{4}{\pi}(J_2 + J_{2,\rm dim})$. The excitation gap appears at $k = \pi/2$ and increases as $4(J_2 - J_{2,\rm dim})\delta$. Note that close to the critical point J_{2c} bosonization yields a very similar form [4,5] $\delta \sim \exp\left(-\frac{{\rm const}J_1}{(J_2 - J_{2c})}\right)$ and a gap which is proportional to δ^2.

For an analysis of the phase diagram we compare the ground state energies of all phases. In the regime of small frustration, the "*AFM+stag.*" solution has the lowest energy and at some point $\alpha_c = J_{2c}/J_1$ crosses with the solution for the dimer state (see Fig. 1 for $\Delta = 1$). This can be identified with a first-order phase transition. Note that at $\Delta = 1$ the "*AFM+uni.*" and the dimer solutions cross very close to an early estimate for the critical point [4] $J_2 = J_1/6$. Taking into account the "*AFM+stag.*" solution shifts this crossing point, thus yielding very good agreement with numerical results [6] $J_{2c} \approx 0.242J_1$ for $\Delta = 1$. Figure 2 shows this crossing point as a function of the anisotropy Δ. Although the critical value of J_2 is very close to numerical results for $\Delta \approx 1$, the position of the crossing decreases with decreasing Δ whereas the exact diagonalization data [18,19] exhibit an increase of J_{2c}.

The excitation gaps of the different mean-field solutions are depicted in Figure 3. The "*uniform*" solution is always gapless and is not displayed. The "*dimer*" and "*AFM+stag.*"solution have a maximum of the gap near

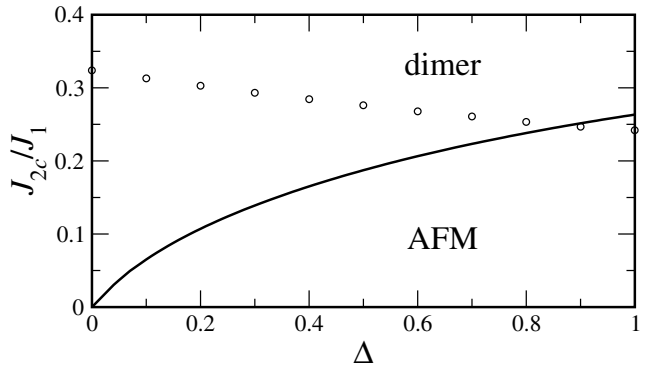

Fig. 2. Phase diagram for the $J_1 - J_2$ XXZ chain as a function of the anisotropy Δ: the solid line is the result of the mean-field approximation, the circles are results of exact diagonalization [19].

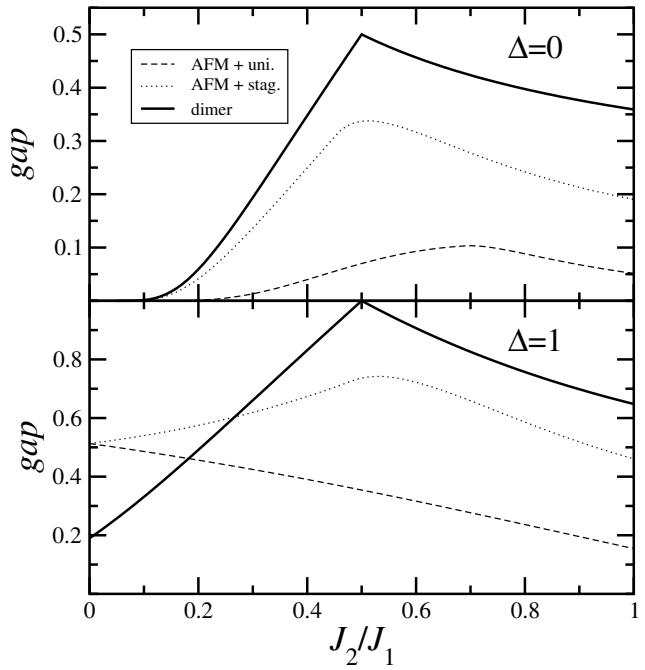

Fig. 3. Excitation gap in the mean-field Hamiltonian as a function of J_2/J_1 for the $J_1 - J_2$ XY chain (upper panel) and the Heisenberg chain (lower panel).

the Majumdar-Ghosh point which is consistent with numerical results [5]. The position of the minimum in the excitation spectrum of the "*dimer*" solution jumps from $k = \pm\pi/2$ to $k = 0$ at the Majumdar-Ghosh point. The minimum of the "*AFM+stag.*" solution shifts continuously for $J_2 > J_1/2$.

The zz-structure factor $S^{zz}(q) = \sum_{l=1}^{L} \exp(iql)\langle s_n^z s_{n+l}^z \rangle$ can be expressed through the four-fermion correlation function. For the dimer state we get the following result in the mean-field approximation:

$$S^{zz}(q) = \frac{1}{4} - \frac{1}{4\pi}\int_0^\pi dk\, \frac{e_k e_{k+q} + f_k f_{k+q}}{\sqrt{(e_k^2 + f_k^2)(e_{k+q}^2 + f_{k+q}^2)}}. \quad (11)$$

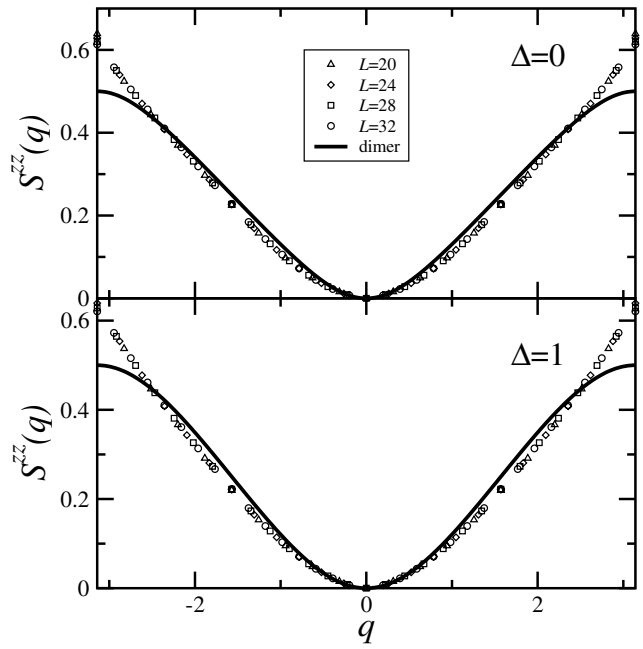

Fig. 4. The structure factor $S^{zz}(q)$ as a function of q for the $J_1 - J_2$ XY chain (upper panel) and Heisenberg chain (lower panel) at $J_2 = 5J_1/11$. The line is the result of the dimer mean-field solution; symbols are exact diagonalization data for different system sizes from 20 to 32 sites.

In the limit of the Majumdar-Ghosh model the exact result [9] $S^{zz}(q) = \frac{1}{4}(1 - \cos(q))$ is recovered. The result (11) for the zz static structure factor at $J_2/J_1 = 5/11$ is shown in Figure 4 as a full line in comparison with numerical results (open symbols). Both approaches yield a broad maximum at the boundary of the Brillouin zone $q = \pm\pi$, signifying antiferromagnetic correlations with a short correlation length [5,9]. Small deviations are observed at $q = \pm\pi$, where the numerical data exhibits also the biggest finite-size effects.

4 Conclusions

To summarize we have applied the Jordan-Wigner transformation to the spin-1/2 $J_1 - J_2$ XXZ chain. We have performed a complete analysis of the possible mean-field states and found that a dimerized state has lowest energy for J_2 larger than some critical value. The ground-state energies are in good agreement with exact diagonalization data and we even recover the exact result at the Majumdar-Ghosh point [7].

The location of the critical point is obtained from the crossing between the energies of the antiferromagnetically ordered state iii) and the dimer state iv). This yields good agreement with numerical results for $\Delta \approx 1$, but does not follow the anisotropy dependence for small Δ correctly. This discrepancy may be related to the following facts. Firstly, spin-spin correlations should decay as a power-law below J_{2c} [4], while the mean-field theory treats this phase

as antiferromagnetically ordered. Secondly, in the mean-field scenario the transition is generically of first order, not of the established infinite order. Just at $\Delta = 0$, we find $J_{2c} = J_{2,\mathrm{dim}} = 0$ and recover the infinite order phase transition to the dimer state, see equation (10).

Furthermore, we have calculated the zz static structure factor for the "*dimer*" mean-field approximation. The result coincides with the exact one for the Majumdar-Ghosh point and satisfactory agreement is found with numerical results in the dimerized phase below the Majumdar-Ghosh point.

It should be mentioned that there are problems with the present approach for large J_2. In particular, the mean-field dimer state does not reveal any incommensurability, as signaled e.g. by a shift of the maxima of the static structure factor beyond the Majumdar-Ghosh point [9]. This is an important difference with reference [16] which obtained incommensurability from a mean-field approach. However, the solution of reference [16] does not correspond to the ground state. Remarkably, the absence of incommensurability is a special property of the dimerized mean-field solution which leads to a cancellation of the next-nearest neighbor hopping processes in the fermionic picture. Consequently, alternative approaches are needed to describe the region $J_2 > J_1/2$.

T.V. would like to thank the Physics Department of the TU Braunschweig for hospitality during the course of this work, and the Deutsche Forschungsgemeinschaft for financial support of this visit. We would like to thank H. Büttner, O. Derzhko, Yu. Gaididei for helpful discussions and G. Bouzerar for communicating his results of a real-space Jordan-Wigner mean-field calculation. Some of the numerical computations have been performed on a COMPAQ ES45 (CFGAUSS) at the Rechenzentrum of the TU Braunschweig.

References

1. T.M. Rice, in *Lecture Notes in Physics*, Vol. 595, edited by C. Berthier, L.P. Lévy, G. Martinez (Springer, 2002)
2. P. Lemmens, G. Güntherodt, C. Gros, Phys. Rep. **375**, 1 (2003)
3. M. Hase, H. Kuroe, K. Ozawa, O. Suzuki, H. Kitazawa, G. Kido, T. Sekine, Phys. Rev. B **70**, 104426 (2004)
4. F.D.M. Haldane, Phys. Rev. B **25**, 4925 (1982)
5. S.R. White, I. Affleck, Phys. Rev. B **54**, 9862 (1996)
6. S. Eggert, Phys. Rev. B **54**, R9612 (1996)
7. C.K. Majumdar, D.K. Ghosh, J. Math. Phys. **10**, 1388 (1969); J. Math. Phys. **10**, 1399 (1969)
8. K. Nomura, J. Phys. Soc. Jpn. **72**, 476 (2003)
9. R. Bursill, G.A. Gehring, D.J.J. Farnell, J.B. Parkinson, T. Xiang, C. Zeng, J. Phys.: Cond. Matt. **7**, 8605 (1995)
10. A.A. Nersesyan, A.O. Gogolin, F.H.L. Eßler, Phys. Rev. Lett. **81**, 910 (1998)
11. D. Allen, D. Sénéchal, Phys. Rev. B **51**, 6394 (1995)
12. A.K. Kolezhuk, Prog. Theor. Phys. Suppl. **145**, 29 (2002)
13. B.S. Shastry, B. Sutherland, Phys. Rev. Lett. **47**, 964 (1981)
14. O. Derzhko, J. Phys. Stud. **5**, 49 (2001)
15. W. Brenig, Phys. Rev. B **56**, 2551 (1997)
16. L. Sun, J. Dai, Sh. Qin, J. Zhang, Phys. Lett. A **294**, 239 (2002)
17. M. Takahashi, *Thermodynamics of One-Dimensional Solvable Models* (Cambridge University Press, 1999)
18. K. Nomura, K. Okamoto, J. Phys. Soc. Jpn. **62**, 1123 (1993); J. Phys. A **27**, 5773 (1994)
19. R.D. Somma, A.A. Aligia, Phys. Rev. B **64**, 024410 (2001)
20. P. Lecheminant, T. Jolicoeur, P. Azaria, Phys. Rev. B **63**, 174426 (2001)
21. M. Zarea, M. Fabrizio, A.A. Nersesyan, Eur. Phys. J. B **39**, 155 (2004)
22. P. Jordan, E. Wigner, Z. Phys. **47**, 631 (1928)
23. E. Fradkin, *Field Theories of Condensed Matter Sytems* (Addison-Wesley, Redwood City, 1991)
24. W.J. Caspers, *Spin Systems* (World Scientific, Singapore, 1989)
25. E. Lieb, T. Schultz, D. Mattis, Ann. Phys. (N.Y.) **16**, 407 (1961)
26. L.N. Bulaevskii, Zh. Eksp. Teor. Fiz. **43**, 968 (1962) [Sov. Phys. JETP **16**, 685 (1963)]
27. T. Hikihara, M. Kaburagi, H. Kawamura, Phys. Rev. B **63**, 174430 (2001)
28. Y. Nishiyama, Eur. Phys. J. B **17**, 295 (2000)
29. H. Büttner, T. Verkholyak, unpublished
30. T. Tonegawa, I. Harada, J. Phys. Soc. Jpn. **56**, 2153 (1987)
31. J.-M. vanden Broeck, L.W. Schwartz, Siam. J. Math. Anal. **10**, 658 (1979)